JOURNAL OF ENVIRONMENTAL SCIENCES 100 (2021) 269–278

Available online at www.sciencedirect.com

ScienceDirect

www.elsevier.com/locate/jes

JES JOURNAL OF ENVIRONMENTAL SCIENCES

www.jesc.ac.cn

Release and sedimentation behaviors of biochar colloids in soil solutions

Qingkang Meng[1,2], *Liang Jin*[1,2], *Leilei Cheng*[1,2], *Jing Fang*[1,4,*], *Daohui Lin*[2,3]

[1] *School of Environmental Science and Engineering, Zhejiang Gongshang University, Hangzhou 310012, China*
[2] *Department of Environmental Science, Zhejiang University, Hangzhou 310058, China*
[3] *Zhejiang Provincial Key Laboratory of Organic Pollution Process and Control, Zhejiang University, Hangzhou 310058, China*
[4] *Key Laboratory of Recycling and Eco-treatment of Waste Biomass of Zhejiang Province, Zhejiang University of Science and Technology, Hangzhou 310023, China*

ARTICLE INFO

Article history:
Received 16 May 2020
Revised 4 August 2020
Accepted 5 August 2020
Available online 14 August 2020

Keywords:
Biochar colloids
Soil solutions
Release
Sedimentation
Stability

ABSTRACT

The release of biochar colloids considerably affects the stability of biochar in environment. Currently, information on the release behavior and suspension stability of biochar colloids in real soil solutions is scarce. In this study, 20 soils were collected from different districts in China and the release behavior of biochar colloids and their suspension stability in soil solutions were systematically examined. The results showed that both pyrolysis temperature and biomass source had important effects on the formation of biochar colloids in soil solutions. The formation amount of biochar colloids from low pyrolysis temperatures (400 °C) (average amount of 9.33–16.41 mg/g) were significantly higher than those from high pyrolysis temperatures (700 °C) (average amount of less than 2 mg/g). The formation amount of wheat straw-derived biochar colloids were higher than those of rice straw-derived biochar colloids probably due to the higher O/C ratio in wheat-straw biochar. Further, biochar colloidal formation amount was negatively correlated with comprehensive effect of dissolved organic carbon, Fe and Al in soil solutions. The sedimentation curve of biochar colloids in soil solutions is well described by an exponential model and demonstrated high suspension stability. Around 40% of the biochar colloids were maintained in the suspension at the final sedimentation equilibrium. The settling efficiency of biochar colloids was positively correlated with comprehensive effect of the ionic strength and K, Ca, Na, and Mg contents in soil solutions. Our findings help promote a deeper understanding of biochar loss and stability in the soil-water environment.

Introduction

Biochar is a carbon material produced via biomass pyrolysis (Ajmal et al., 2020). Its capacities for carbon storage, soil pollutant remediation, and waste recycling have led to its increasingly wide usage in agricultural and environmental fields (Jeffery et al., 2015; Khorram et al., 2017; Fang et al., 2019; Nzediegwu et al., 2020). Biochar can be physically broken in soil through freezing, grinding, thawing, expansion,

* Corresponding author.
E-mails: fangjing@zjgsu.edu.cn (J. Fang), lindaohui@zju.edu.cn (D. Lin).

https://doi.org/10.1016/j.jes.2020.08.002
1001-0742/

and water erosion, thus forming micron and nanometer particles (Spokas et al., 2014;Ravi et al., 2016;Liu et al., 2018b). These broken biochar particles are likely to form highly mobile biochar colloids in solution, a process which causes mass loss and reduces the longevity of biochar's environmental benefits (Hockaday et al., 2007; Jaffé et al., 2013; Liu et al., 2018). Therefore, the release and stability of environmental biochar colloids have received considerable attention in recent years.

In the past decade, the release processes, influencing factors, and colloidal stability of biochar colloids in solutions have been studied. Spokas et al. (2014) pointed out that the absorption of water and water erosion damage the physical structure of biochar, leading to the release of biochar colloids. Liu et al., 2018 found that under the actions of grinding and ultrasound, components with a low degree of carbonization were easily broken and formed biochar colloids. Further, large quantities of biochar colloids can also be released via oscillation treatment (Fang et al., 2020). The preparation temperature of biochar is an important factor affecting the release of biochar colloids in solutions. The colloidal formation amount of biochar prepared through high-temperature pyrolysis (≥ 600 °C) was significantly lower than that of biochar prepared by low- and medium-temperature pyrolysis in NaCl solutions (Liu et al., 2018; Cheng et al., 2020). The abrasion resistance of biochar increases as the pyrolysis temperature increases, leading to a decrease in the content of submicron biochar and formation amount of biochar colloid in solutions (Spokas et al., 2014; Liu et al., 2018; Fang et al., 2020). Biomass source is another important factor impacting the formation amount of biochar colloids in solutions. Liu et al. (2019) reported that the colloids released by woody biochar was lower than that of herb- and fecal-based biochar, mainly due to the high thermal stability of lignin. The formation amount of peanut-shell biochar colloids was lower than that of wheat-straw biochar prepared at the same pyrolysis temperature (Cheng et al., 2020). In addition, the chemistry of the solution also significantly impacts the formation amount and suspension stability of biochar colloids. Increasing the ionic strength of the solution (0.1–20 mmol/L) and decreasing solution pH (3.0–10.0) significantly reduces the biochar colloidal formation amount (Fang et al., 2020). The critical coagulation concentration (CCC) is the minimum electrolyte concentration for rapid agglomeration and deposition of colloids and is a key parameter for evaluating the stability of colloids (Wang et al., 2017). Biochar colloids agglomerate more strongly in bivalent solutions than in univalent solutions (Yang et al., 2019). At a pH of 7.0, the CCCs of biochar colloids in NaCl and $CaCl_2$ solutions were 250 mmo/L and 8.5 mmol/L, respectively (Yi et al., 2015). At a neutral pH, biochar pyrolyzed at low temperatures had a higher colloid stability due to the more negative charge on its surface than that pyrolyzed at high temperatures (Li et al., al.,2017; Liu et al., 2018).

However, the release behavior and suspension stability of biochar colloids were mainly explored in laboratory water/electrolyte solutions in the past, which cannot accurately represent the complexity of natural aqueous solutions. Soil solution formed by soil runoff is an important medium for biochar colloid formation in soil. Due to the diversity of soil types and significant differences in soil properties throughout China, the properties of soil solutions are complex and varied with locations (Lu et al., 2014). Soil particles dispersed by raindrops provide rich matter for slope runoff during rainfall (Wang et al., 2018a). Storm runoff carries complex contaminants such as nutrients, heavy metals, oil, hydrocarbons, pathogens, and salts (Datry et al., 2004; Aryal et al., 2006; Li et al., 2019). To date, however, little information is available on the release behavior and suspension stability of biochar colloids in soil solutions, particularly on the relationship between the properties of soil solutions and the release of biochar colloids.

As an international agricultural center, China is rich in crop straw resources. According to preliminary statistics, China's annual straw production can reach 800 million tons, and the top three straws produced are corn, rice, and wheat straw (Shi et al., 2011; Cao et al., 2019). Biochar can be one of the important ways of straw resource utilization in China. Therefore, wheat and rice straw were used as the biochar sources in this study. We collected cultivated topsoil from 20 different sites in 19 provinces of China and systematically investigated the release behavior and suspension stability of biochar colloids in different soil solutions. The relationship between the properties of soil solutions and biochar colloidal formation amount (and settling properties) was analyzed via systematic clustering, principal component analysis, and correlation analysis. The results of this study will promote an in-depth understanding of the release processes and outcomes of biochar colloids in environmental soil solutions and processes related to biochar loss, thus fostering a more comprehensive understanding of the stability of biochar in natural environments.

1. Materials and methods

1.1. *Preparation and characterization of soil solutions*

As shown in Appendix A **Fig. S1**, 20 cultivated topsoil (0–20 cm) samples were collected from 20 different sites in 19 Chinese provinces and were air-dried and ground to pass through 1-mm Tyler sieves. For soil sampling, 10 soil samples were collected according to S-shaped sampling method in each field and finally mixed 10 parallel samples into one. Soil solutions were prepared with a soil to ultrapure water ratio of 1:15 using 500-mL polyethylene bottles. These mixtures were rotated in a reciprocating shaker (DHZ-C constant temperature oscillator, Suzhou Peiying Experimental Equipment Co., China) at 150 r/min for 24 hr. Then, the soil suspensions were filtered through 0.45 μm membrane filters, and the filtrates was used as the soil solutions. The pH, dissolved organic carbon (DOC) content, and K, Ca, Na, Mg, Fe, and Al contents of the soil solutions were analyzed using a pH meter, a total organic carbon (TOC) analyzer (TOC-VCPH, Shimadzu, Japan), and an inductively coupled plasma atomic emission spectrometer (ICP-AES, SPS 8000 Thermo Fisher Scientific, USA), respectively. The electrical conductivity (EC) of the soil solution was determined using a conductivity meter (Shanghai Precision Scientific Instrument Co. China). The ionic strength (IS) of the soil solution was obtained based on the linear relationship between EC (mS/cm) and IS (M) ($IS = 0.0127 \times EC$) (Morrisson et al., 1990). The soil solutions were analyzed in triplicate.

1.2. Preparation and characterization of biochar

The wheat straw and rice straw were produced in Lianyungang, Jiangsu Province, China. Firstly, washed these straws and dried them at 65 °C. The dried biomass was carbonized under anoxic conditions in a muffle furnace (SX2–12–10, Jinan Precision Scientific Instruments Co., China) at a heating rate of 5 °C /min to the target pyrolysis temperatures (400 or 700 °C), which were maintained for 6 hr. The biochar obtained from the wheat and rice straw pyrolyzed at 400 and 700 °C were labeled as Wheat-BC400, Wheat-BC700, Rice-BC400, and Rice-BC700, respectively. The prepared biochar was ground and sieved through a 100-mesh sieve. The pH of the biochar in ultrapure water (1:50, M/V) was measured using a pH meter. Total C, H, and N contents of biochar were measured with an elemental analyzer (MicroCube, Elementar, Germany), and the O content was determined with the mass balance calculation (Chen et al., 2008a; Liu et al., 2018; Wang et al., 2019). The H/C and (O + N)/C atomic ratios were calculated to evaluate the aromaticity and polarity of the biochar, respectively. The ash content of the biochar was characterized using a thermogravimetric analyzer (TGA, SDTA851, Swrtzer Land, America). All biochar characterizations were performed in triplicate. The wheat-straw biochar used in this experiment was the same used in our previous paper, and its properties are quoted from the published literature (Cheng et al., 2020).

1.3. Extraction of biochar colloids in soil solutions

Biochar (1 g) was added in a 50 mL centrifugal tube containing 48 mL of soil solution and shaken for 24 hr in a thermostatic oscillator at 150 r/min. Afterward, the dispersed suspension was transferred to a 50-mL colorimetric tube and allowed to settle undisturbed at room temperature (25 °C). After settling for 24 h, suspended biochar particles with an size < 2 μm were obtained based on Stokes' law (Tang et al., 2009; Qian et al., 2016; Rosa et al., 2018). For biochar prepared at 400 °C, the suspension was then filtered through a 0.45 μm cellulose acetate membrane. The solid particles retained on the filter membrane were designated as biochar colloids, oven-dried (105 °C) for 24 hr, and weighed to obtain the biochar colloidal formation amount (Fang et al., 2020). To avoid confusion of concepts, in this experiment, biochar colloids specifically refer to biochar particles (0.45–2 μm). Because the colloidal formation amount of biochars prepared at 700 °C is very low in soil solutions, the aforementioned method of drying and weighing is not accurate. Therefore, the biochar colloid concentrations were determined based on the absorbance at 800 nm with a UV–visible spectrophotometer (TU-1901, Beijing Puxi General Instrument Co., Ltd.), and the measured concentrations were converted into biochar colloidal formation amount. The standard concentration curve of the biochar colloids was determined using a stepwise dilution method. In detail, biochar colloids (10 mg) were accurately weighed, and 100 mg/L biochar colloidal suspensions were prepared via ultrasonic dispersion. Then, the gradient dilution method was applied to prepare the standard solution with a concentration gradient of 0–100 mg/L, and its absorbance was determined at 800 nm. Preliminary experimental results showed that the standard concentration curve and the biochar colloid measurements obtained by the stepwise dilution method had a good linear relationship ($R^2 > 0.9998$). All experiments were conducted in triplicate.

1.4. Sedimentation experiments

There are two major processes that can influence the formation amount of biochar colloids in soil solutions: release (during shaking) and sedimentation(during settling) (Fang et al., 2020). To distinguish the effect of soil solution on each process, the sedimentation of biochar colloids was investigated with biochar colloids prepared in advance. Because the formation amount of biochar colloids prepared at high pyrolysis temperatures (700 °C, BC700) was very low, sedimentation experiments were only conducted for biochar colloids prepared at low pyrolysis temperatures (400 °C, BC400). Biochar (1 g) was added to a 50 mL centrifugal tube containing 48 mL of ultrapure water, and the biochar colloids were obtained via the method described in Section 1.3. The sedimentation of biochar colloids was studied in various soil solutions. Briefly, biochar colloids (5 mg) were sonicated (100 W, 40 kHz, 25 °C, 30 min) with soil solutions (50 mL) in colorimetric tubes, after that 2 mL suspensions were immediately transferred into a quartz cuvette for settling. After settling for 0, 4, 6, 8, 10, 12, and 24 hr, the absorbance of unsettled fraction of biochar colloids was measured at 800 nm during 24 hr (TU-1901, Beijing Puxi General Instrument Co., Ltd.), which was finally quantified as the ratio of absorbance (A) at 4 hr (A_4), 6 hr (A_6), 8 hr (A_8), 10 hr (A_{10}), 12 hr (A_{12}), and 24 hr (A_{24}) to that at 0 hr (A_0) (Ma et al., 2015). The hydrodynamic diameter of the biochar colloids after settling for 0 and 24 hr were measured by Zetasizer (Nano ZS90, Malvern Instrument Ltd., UK). All treatments were conducted in two duplicates. The settling curves of the biochar colloids in soil solutions were fitted with an exponential model expressed as follows (Luan et al., 2014):

$$y = y_0 + P\exp(-R_0 t) \quad (1)$$

where t is the settling time, y is A/A_0 at time t, y_0 is the equilibrium A/A_0, P is the decreased A/A_0 at the equilibrium, and R_0 is the sedimentation rate.

1.5. Data analysis

All experimental data were expressed as the mean of repetitions, and the figures were drawn using Origin 2018. Statistical analyses such as system clustering, principal component analysis, and correlation analysis were performed using IBM SPSS Statistics 20.

2. Results and discussion

2.1. Biochar characteristics

The pH, ash content, element content, and atomic ratio of the investigated biochars are summarized in Table 1. The pH values of Wheat-BC400 and Rice-BC400 were 6.6 and 7.7, respectively, which increased to strong alkalinity (pH > 10) as the pyrolysis temperature increased to 700 °C for Wheat-BC700 and

Table 1 – Physicochemical properties of biochar.

Biochar	pH	Ash (%)	Elemental content (%)				Atomic ratio		
			C	H	O	N	H/C	O/C	(O + N)/C
Wheat-BC400	6.6	14.3	59.6	3.1	22.1	0.9	0.62	0.28	0.29
Rice-BC400	7.7	22.2	56.0	3.1	17.1	1.6	0.66	0.23	0.25
Wheat-BC700	10.2	18.7	67.3	1.5	11.8	0.7	0.27	0.13	0.14
Rice-BC700	10.4	26.5	59.0	1.8	11.5	1.2	0.37	0.15	0.16

Rice-BC700. High pyrolysis temperatures promote the decomposition of carboxyl groups, phenolic hydroxyl groups, and other acidic functional groups and the volatilization of organic acids, thus increasing biochar alkalinity (Rosa et al., 2018; Liu et al., 2018; Li et al., 2018). When the pyrolysis temperature increased from 400 to 700 °C, the C content in wheat-straw and rice-straw biochar increased from 59.6% and 56.0% to 67.3% and 59.0%, respectively, and the ash content increased from 14.3% and 22.2% to 18.7% and 26.5%, respectively. However, the H content decreased from 3.1% and 3.1% to 1.5% and 1.8%, respectively, and the O content decreased from 22.1% and 17.1% to 11.8% and 11.5%, respectively. Accordingly, the H/C and O/C values of biochar pyrolyzed at 700 °C were significantly lower than those of biochar pyrolyzed at 400 °C. The decrease in the H/C ratio means that the amount of aromatic carbon in the biochar increases (Qian et al., al.,2016; Ma et al., 2017). The larger the O/C and (O + N)/C ratios, the greater the hydrophilicity and polarity of the biochar (Chen et al., al.,2008a, Chen et al., 2008; Lin et al., al.,2007; Ma et al., 2017). Thus, the hydrophilicity and polarity of biochar prepared at 400 °C were higher than those obtained at 700 °C, while the aromatic carbon content and hydrophobicity of biochar prepared at 700 °C were higher than those obtained via 400 °C pyrolysis. In addition, the properties of biochar from different biomass sources varied greatly. For example, when the pyrolysis temperature was 400 °C, the O, O/C, and (O + N)/C contents in wheat-straw biochar were all greater than those in rice-straw biochar, indicating that the hydrophilicity and polarity of wheat-straw biochar were greater than those of rice-straw biochar. The ash content of rice-straw biochar prepared at 400 and 700 °C (22.2% and 26.5%, respectively) was higher than that of wheat-straw biochar prepared at both pyrolysis temperatures (14.3% and 18.7%).

2.2. *Soil-solution properties*

The physical and chemical properties of the soil solutions, which varied greatly, are shown in Table 2. The pH of the soil solutions ranged from 5.3–8.9. The DOC content ranged from 35.1 to 153.4 mg/L, with an average value of 91.1 mg/L. Ionic strength ranged from 0.2–7.7 mmol/L, with an average of 3.2 mmol/L. The concentrations of monovalent K and Na cations ranged from 6.23 to 13.78 mg/L and 1.17 to 21.53 mg/L, respectively. The divalent Ca and Mg cation contents ranged from not detected (ND)–38.75 mg/L and ND–15.70 mg/L, respectively. Fe and Al contents ranged from ND–0.34 mg/L and 0.01–0.64 mg/L, respectively.

As shown in Fig. 1**a**, through the system clustering of soil-solution properties, the 20 soil solutions could be divided into four categories. The clustering genealogy map shows that the AS soil solution (collected from Anshan, China) is in a class unto itself, constituting the first cluster. The soil sampling sites included in the second cluster were the Hangzhou (HZ), Hengyang (HY), Jiujiang (JJ) and Nanjing (NJ) sites. The soil sampling sites included in the third cluster were Harbin (HEB), Chifeng (CF), Jilin (JL), Haibei Tibetan Autonomous Prefecture (HBZZ), Zhaotong (ZT), Tianjin (TJ), Maoming (MM), Hulun Buir (HLBE), Dongying (DY) and Chongqing (CQ). Finally, the fourth cluster included the Quzhou (QZ), Yingtan (YT), Taiyuan (TY), Jiuquan (JQ) and Ledong Li Autonomous County (LDLZ) sites. To eliminate redundant information contained in the correlation between variables (Fang et al., 2009), we conducted a principal component analysis of the soil-solution properties. As shown in Fig. 1**b**, three principal components were obtained from the 20 soil solutions. The first principal component was mainly related to IS and K, Ca, Na, and Mg content, which explained 42.6% of the variation. The second principal component was mainly related to the DOC, Fe, and Al contents, explaining 25.2% of the variation. The third principal component was mainly related to pH and explained 12.1% of the variation. As shown in Table 2, the bivalent cationic Ca and Mg contents in the soil solution of the first cluster were the highest among the 20 soil solutions and were 38.75 mg/L and 15.70 mg/L, respectively. Moreover, the IS and monovalent cation (K, Na) content were also very high, twice the average values of the corresponding indexes (IS, K, and Na) of the 20 soil solutions. The DOC, Fe, and Al contents in the soil solutions of the second cluster were higher than the overall averages (approximately 10% higher). The DOC, K, Fe, and Al contents in the soil solutions in the third cluster were close to the average values of the corresponding indexes (DOC, K, Fe, Al) for the 20 soil solutions tested. Finally, The IS, DOC, K, Ca, Na, Fe, and Al contents in the soil solutions of the fourth cluster were relatively low, and their mean values were all lower than that of the average values of the 20 tested soil solutions.

2.3. *Formation amount of biochar colloids in soil solutions*

The formation amount of biochar colloids in different soil solutions are shown in Fig. 2. The colloidal formation amount of BCs prepared at different pyrolysis temperatures were significantly different. The average colloidal formation amount of biochars prepared via low-temperature pyrolysis (400 °C) were

Table 2 – Physicochemical properties of soil solutions.

Site	Serial number	Soil classification	pH	IS (mmol/L)	DOC (mg/L)	Metal element concentrations in soil solutions (mg/L)					
						K	Ca	Na	Mg	Fe	Al
Hulunbuir	HLBE	chernozem	8.2	3.9	108.8	6.77	9.65	18.91	1.30	0.12	0.28
Harbin	HEB	meadow soil	7.5	3.7	86.9	8.69	15.56	1.75	0.59	0.05	0.15
Jilin	JL	brown soil	6.9	2.2	93.0	7.29	11.81	3.14	1.58	0.004	0.11
Anshan	AS	brown soil	6.6	7.2	66.3	13.78	38.75	13.46	15.70	ND	0.01
Tianjin	TJ	hydric soil	7.5	6.0	78.1	8.11	20.98	2.82	3.91	ND	0.01
Chifeng	CF	chestnut soil	7.4	2.1	87.7	7.43	14.69	2.54	1.51	ND	0.05
Dongying	DY	saline soil	7.8	4.3	88.0	9.27	9.28	21.53	2.57	ND	0.08
Taiyuan	TY	cinnamon soil	8.9	1.4	62.0	6.59	9.43	2.19	2.00	ND	0.02
Jiuquan	JQ	brown desert soil	8.9	2.0	68.7	6.57	4.20	2.10	1.97	0.11	0.21
Nanjing	NJ	paddy soil	7.5	2.7	153.4	6.51	11.61	1.89	0.71	0.34	0.59
Hangzhou	HZ	paddy soil	7.9	2.4	126.9	7.35	11.43	1.73	0.42	0.08	0.28
Quzhou	QZ	red soil	5.3	1.7	56.7	6.37	ND	1.28	ND	ND	0.04
Jiujiang	JJ	yellow brown soil	7.1	1.6	137.8	6.74	3.85	1.60	ND	0.34	0.64
Yingtan	YT	red soil	6.9	0.2	54.1	6.23	ND	1.17	ND	ND	0.06
Hengyang	HY	purple soil	7.4	3.9	128.5	7.70	14.28	2.44	0.30	0.16	0.55
Zhaotong	ZT	yellow soil	7.6	7.7	96.1	6.60	23.35	2.73	2.50	0.02	0.13
Chongqing	CQ	calcareous soil	6.4	0.4	102.8	6.42	ND	1.25	ND	0.16	0.26
Maoming	MM	laterite	7.4	6.3	78.2	9.12	17.84	3.51	1.57	ND	0.09
Ledong Li Autonomous County	LDLZ	yellow soil	7.8	2.0	35.1	6.30	0.10	1.22	ND	0.01	0.21
Tibetan Autonomous Prefecture of Haibei	HBZZ	chernozem	7.8	2.1	92.6	10.93	12.23	2.49	1.26	0.03	0.12

ND: not detected; DOC: dissolved organic carbon; IS: ionic strength.

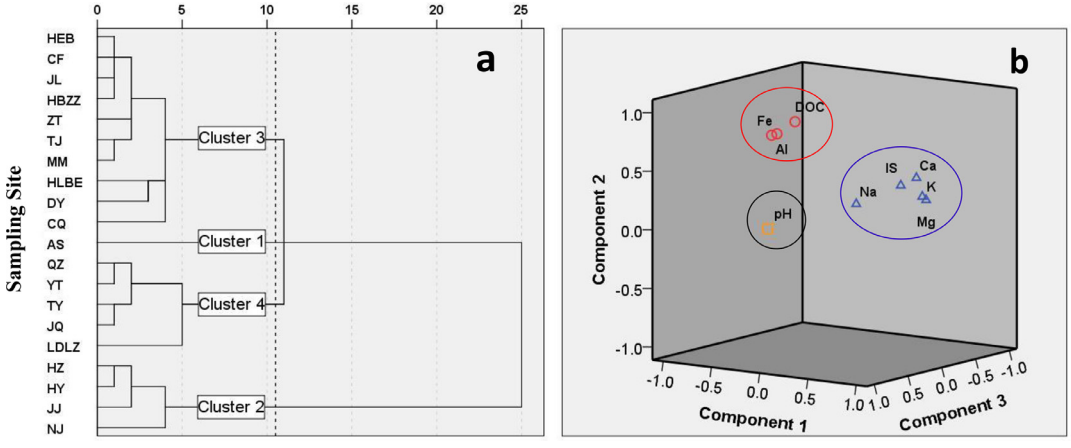

Fig. 1 – Principal component analysis of the properties of soil solutions. (a) Cluster pedigree diagram and (b) principal component. Sampling site: HEB=Harbin, CF=Chifeng, JL=Jilin, HBZZ=Tibetan Autonomous Prefecture of Haibei, ZT=Zhaotong, TJ=Tianjin, MM=Maoming, HLBE=Hulunbuir, DY=Dongying, CQ=Chongqing, AS=Anshan, QZ=Quzhou, YT=Yingtan, TY=Taiyuan, JQ=Jiuquan, LDLZ=Ledong Li Autonomous County, HZ=Hangzhou, HY=Hengyang, JJ=Jiujiang, NJ=Nanjing.

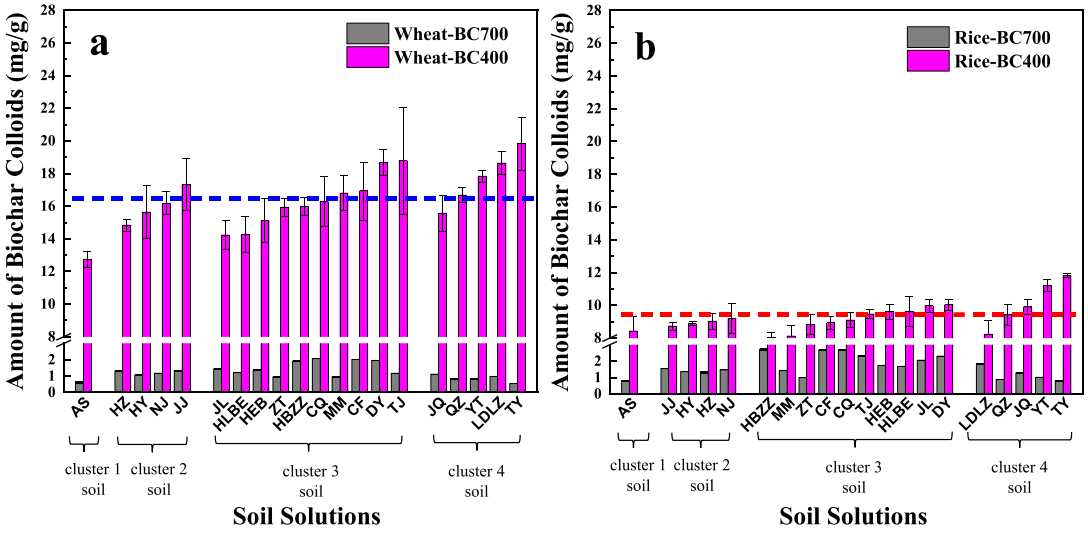

Fig. 2 – The formation amount of biochar colloids in various soil solutions. (a) Wheat-straw biochar; (b) rice-straw biochar. Soil Sampling Site: AS=Anshan, JL=Jilin, HLBE=Hulunbuir, HZ=Hangzhou, HEB=Harbin, JQ=Jiuquan, HY=Hengyang, ZT=Zhaotong, HBZZ=Tibetan Autonomous Prefecture of Haibei, NJ=Nanjing, CQ=Chongqing, QZ=Quzhou, MM=Maoming, CF=Chifeng, JJ=Jiujiang, YT=Yingtan, LDLZ=Ledong Li Autonomous County, DY=Dongying, TJ=Tianjin, TY=Taiyuan. The dotted blue line in Fig. 2a represents the average amount of Wheat-BC400 colloid in 20 soil solutions (16.41 mg/g). The dotted red line in Fig. 2b represents the average amount of Rice-BC400 colloids in 20 soil solutions (9.33 mg/g).

significantly higher than those from high-temperature pyrolyzed BCs (700 °C) in soil solutions. The average colloidal formation amount (16.41 mg/g) of Wheat-BC400 was 13.2 times higher than that of Wheat-BC700 (1.24 mg/g). Similarly, the average colloidal formation amount (9.33 mg/g) of Rice-BC400 was 5.7 times higher than that of Rice-BC700 (1.64 mg/g). This result is consistent with those of previous studies, in which biochar prepared at lower pyrolysis temperatures more readily formed biochar colloids (Liu et al., 2018; Cheng et al., 2020; Fang et al., 2020). In the pyrolysis temperature range of 300–700 °C, biochar prepared at low pyrolysis temperatures can more easily be physically decomposed than biochar prepared at high pyrolysis temperatures in solutions, and the colloidal formation amount is positively correlated with the biochar O/C value (Spokas et al., 2014; Liu et al., 2018; Song et al., 2019). The structure and hardness of the graphite microcrystals of biochar prepared at a high pyrolysis temperature enhance its resistance to abrasion and reduce the probability of its physical decomposition (Braadbaart et al., 2009; Naisse et al., 2015; Cheng et al., 2020; Fang et al., 2020). Notably, the colloidal formation amount of biochar prepared at 700 °C are very low (less than 2 mg/g) in soil solutions; thus, the mass loss and environmental risk associated with colloidal loss are very low for such biochars. Furthermore, the colloidal formation amount of biochar from different biomass sources also vary greatly in soil solutions. For example, the average colloidal formation amount of Wheat-BC400 in the 20 examined soil solutions (16.41 mg/g) was 1.8 times higher than that of Rice-BC400 (9.33 mg/g). This may be related to the higher O/C ratio in wheat-straw biochar. Previous studies found that O/C of biochar were positively correlated with colloidal formation amount of biochar in aqueous solutions (Liu et al., 2018; Song et al., 2019).

2.4. *Relationship between soil-solution properties and formation amount of biochar colloids*

The release behavior of biochar colloids is not only influenced by the properties of the biochar itself but also by the chemical properties of the solutions (Liu et al., 2018; Cheng et al., 2020; Fang et al., 2020). Higher IS and lower pH in soil solutions could significantly inhibit biochar colloidal formation amount (Fang et al., 2020). The formation amount of biochar colloids in the soil solutions of the first cluster were significantly lower than the average amount across the 20 tested soil solutions. Specifically, the colloidal formation amount were decreased by 22.4%, 9.6%, 50.7%, and 51.9% for Wheat-BC400, Rice-BC400, Wheat-BC700, and Rice-BC700, respectively, comparing to the average amount. This may be related to the higher IS and K, Ca, Na, and Mg contents in the first soil-solution cluster.

We attempted to establish the correlation between the colloidal formation amount of biochar and individual properties of soil solutions. However, the results of a Pearson correlation analysis showed that no significant correlation existed between colloidal formation amount of biochar and individual soil-solution properties, indicating that the release behavior of biochar colloids in soil solutions is affected by multiple soil-solution properties acting in combination. Similar results were found in previous studies. For example, the stability of colloidal nanomaterials in natural water is affected by the comprehensive characteristics of the water (Keller et al., 2010; Quik et al., 2014). A correlation analysis between the principal component score of an original variable and an object can reveal the relationship between the object and original variable (Li et al., 2016). Therefore, we analyzed the correlation between the colloidal formation amount of biochar and the three principal components of the soil-solution prop-

Table 3 – Pearson correlation coefficient between the three principal components describing the properties of soil solutions with the biochar colloid yields (Y) and the P value of the exponential model fitting parameter.

Pearson correlation analysis		Component 1	Component 2	Component 3
$Y_{Wheat-BC400}$	correlation coefficient	−0.254	−0.449**	0.252
	p	0.280	0.047	0.283
$Y_{Rice-BC400}$	correlation coefficient	−0.147	−0.398*	0.329
	p	0.535	0.082	0.156
$P_{Wheat-BC400}$	correlation coefficient	0.441*	−0.082	−0.081
	p	0.067	0.745	0.751
$P_{Rice-BC400}$	correlation coefficient	−0.288	0.340	0.202
	p	0.246	0.167	0.422

(−) represents negative correlation; * represents significance level $p < 0.1$; ** represents significance level $p < 0.05$.

erties, and the results are shown in Table 3. Because the colloidal formation amount of biochar prepared at 700 °C were very low in soil solutions, we focused only on the biochar prepared at 400 °C. As shown in Table 3, the colloidal formation amount of Wheat-BC400 and Rice-BC400 were negatively correlated with the second principal component, indicating that the formation amount of biochar colloids is closely related to the DOC, Fe, and Al contents in soil solutions. Fe and Al in soil solutions exist in the form of iron hydroxide and aluminum hydroxide colloids via the coordination of hydroxyl groups (Xu et al., 2001). Iron and aluminum colloids are often positively charged, which is conducive to the agglomeration and deposition of biochar colloidal particles with negative surface charge. Moreover, iron and aluminum oxides can exchange with the mineral surface through hydroxyl or carboxyl groups on the surface of humus and form stable organo-inorganic complexes with humic acid and fulvic acid (Hou et al., al.,2007; Nagao, 2005; Wang et al., 2016, Wang et al., 2018). These organo-inorganic complexes can promote the agglomeration of biochar colloids and eventually reduce colloidal formation amount in soil solutions. The above correlation analysis results are consistent with the experimental results. For example, the DOC, Fe, and Al contents in the soil solutions of the second cluster were relatively high. Accordingly, the colloidal formation amount of Wheat-BC400 and Rice-BC400 in the second soil-solution cluster were lower than the average value in the 20 soil solutions tested. The DOC, Fe, and Al contents in the soil solutions of the third cluster were close to the average values of the 20 soil solutions tested. Accordingly, the colloidal formation amount of Wheat-BC400 and Rice-BC400 in the third-cluster soil solutions were also close to the average amount. The DOC and Fe contents in the fourth-cluster soil solutions were relatively low. Accordingly, the colloidal formation amount of Wheat-BC400 and Rice-BC400 in the fourth-cluster soil solutions were higher than the average amount within all tested soil solutions.

2.5. *Sedimentation behavior of biochar colloids in soil solutions*

The sedimentation curves of the biochar colloids and their exponential model fitting curves in various soil solutions are shown in Fig. 3. In most soil solutions, the biochar colloids settled slowly within 24 hr, which is consistent with their final small aggregate sizes. As shown in Fig. 3, after aggregating for 24 hr, the hydrodynamic diameter (D_{24hr}) of Wheat-BC400 and Rice-BC400 biochar colloids in various soil solutions were 387–490 nm and 450–588 nm, respectively, which were just a little larger than their initial size (increased by less than 20%). The P value of the model fitting parameter represents the A/A_0 reduction at the sedimentation equilibrium. The larger P values indicate that more biochar colloid particles will eventually settle and that the colloids will be more unstable in soil solutions. The average P values of Wheat-BC400 and Rice-BC400 colloids in the 20 tested soil solutions were 0.599 and 0.569, respectively; in other words, 59.9% and 56.9% of the biochar colloidal particles eventually aggregated and settled, while nearly 40% of the biochar colloids remained suspended and stable. Previous studies have shown that after 10 days, more than 98% of TiO_2 nanoparticles in soil suspensions settled, and only 1.17%–2.83% of the particles remained suspended (Fang et al., 2009). In seawater with low TOC content and high IS, the deposition rate of metal oxide nanoparticles (TiO_2, ZnO, and CeO_2) is very high, and at least 70% of nanoparticles aggregate and settle after 3 hr (Keller et al., 2010). More than 90% of fullerene (C_{60}) nanoparticles settled after 15 days in all tested water samples (seawater, river, lake) (Quik et al., 2014). After 14 days of settling in natural water (river water), more than 80% of ZnO nanoparticles settled and less than 20% remained suspended, while nearly all TiO_2 nanoparticles settled (Fang et al., al.,2017). Therefore, compared with nanomaterials, biochar colloids have stronger suspension stability in natural solutions.

To better understand the relationship between the properties of the soil solutions and of biochar colloidal sedimentation, we analyzed the correlation between the P values of the exponential model fitting parameter and the three principal components describing the soil-solution properties. According to Table 3, only the P value of Wheat-BC400 had a significant positive correlation with the first principal component, while that of Rice-BC400 had no significant correlation. The first principal component was mainly related to the IS, K, Ca, Na, and Mg contents, indicating that the sedimentation behavior of Wheat-BC400 is largely related to the aforementioned soil-solution properties. Higher IS and divalent cation content in the soil solution were associated with increased colloid agglomeration (Bradford et al., 2010;Keller et al., 2010). The above correlation analysis results are consistent with the experimental results. For example, in the first soil-solution cluster, which had the highest Ca and Mg content, high IS,

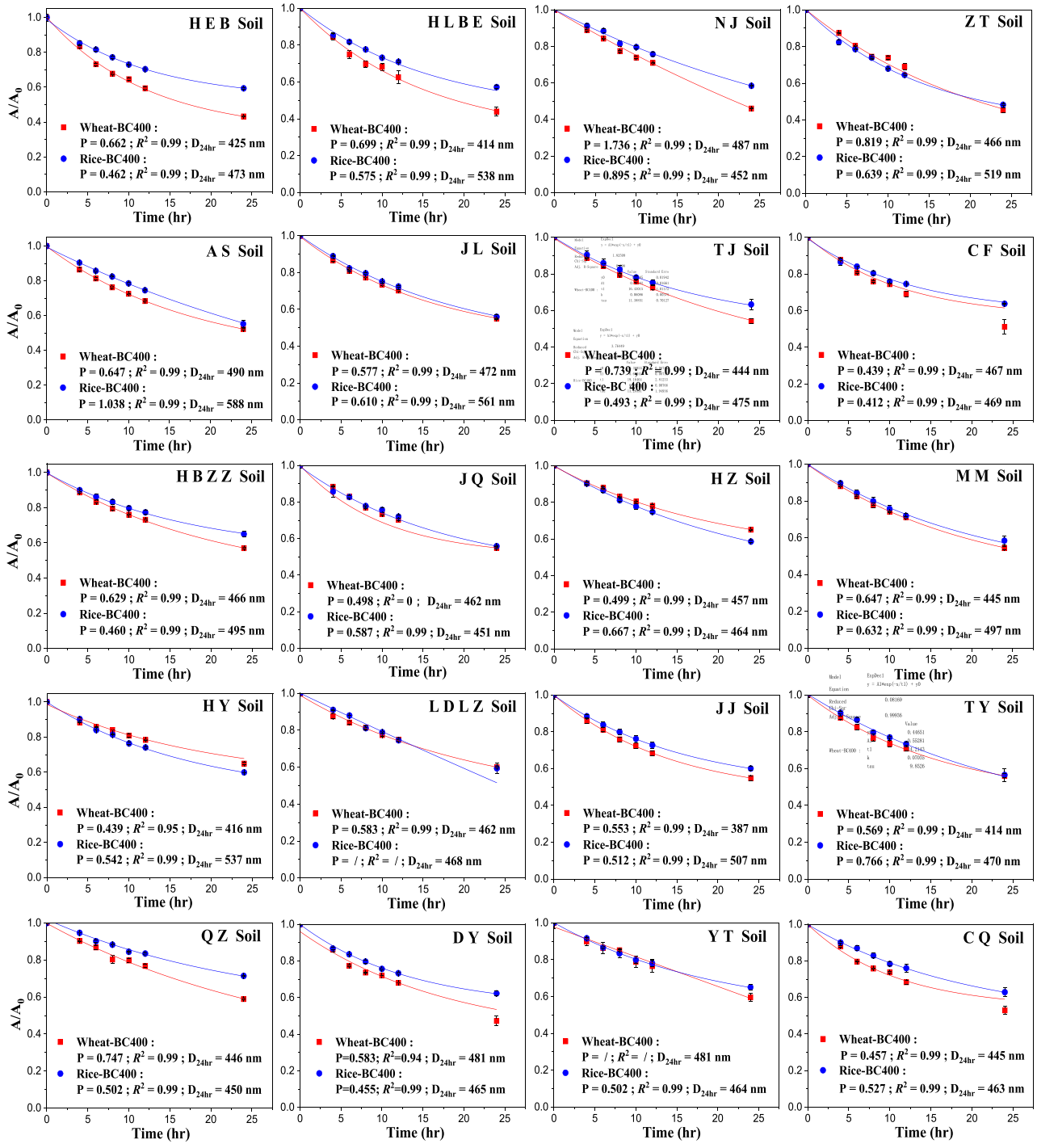

Fig. 3 – Sedimentation curves of biochar colloids and exponential model fitting curves in various soil solutions. P represents the A/A_0 reduction at the settlement equilibrium. D_{24hr} is the hydrodynamic diameter of the biochar colloids after settling for 24 hr. / indicates that the sedimentation curve is not applicable to the model fitting equation. Soil Sampling Site: HEB=Harbin, HLBE=Hulunbuir, NJ=Nanjing, ZT=Zhaotong, AS=Anshan, JL=Jilin, TJ=Tianjin, CF=Chifeng, HBZZ=Tibetan Autonomous Prefecture of Haibei, JQ=Jiuquan, HZ=Hangzhou, MM=Maoming, HY=Hengyang, LDLZ=Ledong Li Autonomous County, JJ=Jiujiang, TY=Taiyuan, QZ=Quzhou, DY=Dongying, YT=Yingtan, CQ=Chongqing.

and high monovalent cation (K, Na) content, the P value of the Wheat-BC400 sedimentation parameter was 0.647, which was higher than the average value for the 20 tested soil solutions (0.599). The P value of the Rice-BC400 sedimentation parameter was around 1.0 (1.038), indicating that Rice-BC400 will eventually settle completely in the first soil-solution cluster. Overall, this indicates that the biochar colloids are very unstable in the first soil-solution cluster.

3. Conclusions

The release behavior and suspension stability of biochar colloids were investigated in 20 different soil solutions in this study. Both the pyrolysis temperature and biomass source had an important effect on the formation amount of biochar colloids in soil solutions. The formation amount of biochar colloids from low temperature (400 °C) was significantly higher (more than five times) than that from high temperature (700 °C) in soil solutions. For biochars prepared at the same pyrolysis temperature, the formation amount of wheat-straw biochar colloids was higher than that of rice-straw biochar colloids in soil solutions because of the higher O/C ratio in wheat-straw biochar. The formation amount of biochar colloids was negatively correlated with the comprehensive effect of the levels of DOC, Fe ions, and Al ions in soil solutions. The formation amount of biochar colloids from high temperature (700 °C) was very low (average amount of less than 2 mg/g), indicating that the mass loss and environmental risk due to biochar colloidal loss were very low. The suspension stability of biochar colloids prepared at 400 °C was very high in the soil solutions; nearly 40% of the biochar colloids remained stable at sedimentation equilibrium. The settling efficiency of biochar colloids was positively correlated with comprehensive effect of the ionic strength and K, Ca, Na, and Mg contents in soil solutions. As the stability of biochar in soil determines the level of associated environmental risk, our results suggest that the carbon loss of biochar derived via low-temperature pyrolysis in the form of colloids cannot be neglected. Further, the risk of biochar colloids migration should also be an area of focus due to the strong suspension stability of biochar colloids.

Acknowledgements

This work was supported by the National Natural Science Foundation of China (Nos. 21976158 and 21677129).

Appendix A Supplementary data

Supplementary material associated with this article can be found, in the online version, at doi:10.1016/j.jes.2020.08.002.

REFERENCES

Ajmal, Z., Muhmood, A., Dong, R., Wu, S., 2020. Probing the efficiency of magnetically modified biomass-derived biochar for effective phosphate removal. J. Environ. Manag. 253.

Aryal, R.K., Murakami, M., Furumai, H., Nakajima, F., Jinadasa, H.K.P.K., 2006. Prolonged deposition of heavy metals in infiltration facilities and its possible threat to groundwater contamination. Water Sci. Technol. 54 (6–7), 205–212.

Braadbaart, F., Poole, I., van Brussel, A.A., 2009. Preservation potential of charcoal in alkaline environments: an experimental approach and implications for the archaeological record. J. Archaeol. Sci. 36 (8), 1672–1679.

Bradford, S.A., Kim, H., 2010. Implications of cation exchange on clay release and colloid-facilitated transport in porous media. J. Environ. Qual. 39 (6), 2040–2046.

Chen, B., Zhou, D., Zhu, L., 2008a. Transitional adsorption and partition of nonpolar and polar aromatic contaminants by biochars of pine needles with different pyrolytic temperatures. Environ. Sci. Technol. 42 (14), 5137–5143.

Chen, B., Zhou, D., Zhu, L., Shen, X., 2008. Adsorption of organic pollutants in water by biological carbon adsorbent and its mechanism. Scientia Sinica(Chimica) 38 (6), 530–537 (in Chinese).

Cheng, L., Meng, Q., Jin, L., Yang, Y., Fang, J., Lin, D., 2020. Influence of pyrolysis temperature and ionic strength on the release behavior of biochar colloid from different feedstocks. Acta Scien. Circum doi:10.13671/j.hjkxxb.2019.0452, (in Chinese).

Cao, Y., Chen, X., Sha, Z., Dong, Y., Yuan, J., Cao, L., 2019. Effect of rice straw returning on accumulation of heavy metals in soil and yield of wheat. J. Shanghai Jiaotong University(Agr. Sci.) doi:10.3969/J.ISSN.1671-9964.2019.04.002, (in Chinese).

Datry, T., Malard, F., Gibert, J., 2004. Dynamics of solutes and dissolved oxygen in shallow urban groundwater below a stormwater infiltration basin. Sci. Total Environ. 329 (1–3), 215–229.

Fang, J., Jin, L., Cheng, L., Lin, D., 2019. Advancement in research on stability of biochar in the environment. Acta Pedologica Sinica 56 (5), 1035–1047 (in Chinese).

Fang, J., Cheng, L., Rashida, H., Jin, L., Wang, D., Owens, G., et al., 2020. Release and stability of water dispersible biochar colloids in aquatic environments: effects of pyrolysis temperature, particle size, and solution chemistry. Environ. Pollut. doi:10.1016/j.envpol.2020.114037.

Fang, J., Shan, X., Wen, B., Lin, J., Owens, G., 2009. Stability of titania nanoparticles in soil suspensions and transport in saturated homogeneous soil columns. Environ. Pollut. 157 (4), 1101–1109.

Fang, J., Shijirbaatar, A., Lin, D., Wang, D., Shen, B., Sun, P., et al., 2017. Stability of co-existing ZnO and TiO2 nanomaterials in natural water:aggregation and sedimentation mechanisms. Chemosphere 184, 1125–1133.

Hou, T., Xu, R., Zhao, A., 2007. Interaction between electric double layers of kaolinite and Fe/AI oxides in suspensions. Colloid Surf. A 297, 91–94.

Hockaday, W.C., Grannas, A.M., Kim, S., Hatcher, P.G., 2007. The transformation and mobility of charcoal in a fire-impacted watershed. Geochim. Cosmochim. Ac. 71 (14), 3432–3445.

Jaffé, R., Ding, Y., Niggemann, J., Vähätalo, A.V., Stubbins, A., Spencer, R.G.M., et al., 2013. Global charcoal mobilization from soils via dissolution and riverine transport to the oceans. Science 340 (6130), 345–347.

Jeffery, S., Bezemer, T.M., Cornelissen, G., Kuyper, T.W., Lehmann, J., Mommer, L., et al., 2015. The way forward in biochar research: targeting trade-offs between the potential wins. GCB Bioenergy 7 (1), 1–13.

Keller, A.A., Wang, H., Zhou, D., Lenihan, H.S., Cherr, G., Cardinale, B.J., et al., 2010. Stability and aggregation of metal oxide nanoparticles in natural aqueous matrices. Environ. Sci. Technol. 44 (6), 1962–1967.

Khorram, M.S., Lin, D., Zhang, Q., Zheng, Y., Fang, H., Yu, Y., 2017. Effects of aging process on adsorption–desorption and bioavailability of fomesafen in an agricultural soil amended with rice hull biochar. J. Environ. Sci. 56, 180–191.

Liu, G., Zheng, H., Jiang, Z., Wang, Z., 2018b. Effects of biochar input on the properties of soil nanoparticles and dispersion/sedimentation of natural mineral nanoparticles in aqueous phase. Sci. Total Environ. 634, 595–605.

Liu, C., Chu, W., Li, H., Stephen, A.B., Brian, J.T., Mao, J., Johannes, L., Zhang, W., 2019. Quantification and characterization of dissolved organic carbon from biochars. Geoderma 335, 161–169.

Luan, Y., Jing, L., Wu, J., Xie, M., Feng, Y., 2014. Long-lived photogenerated charge carriers of 001-facet-exposed TiO_2 with enhanced thermal stability as an efficient photocatalyst. Appl. Catal. B-Environ. 147, 29–34.

Lin, D., Pan, B., Zhu, L., Xing, B., 2007. Characterization and phenanthrene sorption of tea leaf powders. J. Agr. Food. Chem. 55 (14), 5718–5724.
Li, H., Dong, X., da Silva, E.B., de Oliveira, L.M., Chen, Y., Ma, L., 2017. Mechanisms of metal sorption by biochars: biochar characteristics and modifications. Chemosphere 178, 466–478.
Li, H., Jia, B., Cheng, B., Guo, C., Li, J., 2019. Research progress on the effect of concentrated runoff infiltration on soil and groundwater in sponge city. Adv. Water Sci. doi:10.14042/j.cnki.32.1309.2019.04.014, (in Chinese).
Liu, G., Zheng, H., Jiang, Z., Zhao, J., Wang, Z., Pan, B., et al., 2018. Formation and physicochemical characteristics of nano biochar: insight into chemical and colloidal stability. Environ. Sci. Technol. 52 (18), 10369–10379.
Lu, S., Wang, Y., He, L., 2014. Soil environmental quality survey and monitoring in China. Environ. Monit. China doi:10.19316/j.issn.1002-6002.2014.06.003, (in Chinese).
Li, J., Gu, K., Tang, C., Wang, H., Shi, B., 2018. Advances in effects of biochar on physical and chemical properties of soils. J. Zhejiang Univ. (Eng. Sci.) doi:10.3758/j.issn.1008-973X.2018.01.025, (in Chinese).
Li, X., Zhu, J., Wang, X., Dong, X., 2016. Analysis of influencing factors of grain output in Henan province based on principal component analysis. J. Henan Agr. Univ. 50 (2), 269–274 (in Chinese).
Morrisson, A.R., Park, J.S., Sharp, B.L., 1990. Application of high-performance sizeexclusion liquid chromatography to the study of copper speciation in waters extracted from sewage sludge treated soils. Analyst 115, 1429–1433.
Ma, S., Zhou, K., Yang, K., Lin, D., 2015. Hetero-agglomeration of oxide nanoparticles with algal cells: effects of particle type, ionic strength and pH. Environ. Sci. Technol. 49 (2), 932–939.
Ma, F., Zhao, B., 2017. Sorption of p-Nitrophenol by biochars of corncob prepared at different pyrolysis temperature. Environ. Sci. 38 (2), 838–844 (in Chinese).
Nagao, S., 2005. Transport of biogeochemical materials from the Amur river to the sea of Okhotsk. Japan: Report on Amur-Okhotsk Project. 67-69.
Naisse, C., Girardin, C., Lefevre, R., Pozzi, A., Maas, R., Stark, A., et al., 2015. Effect of physical weathering on the carbon sequestration potential of biochars and hydrochars in soil. GCB Bioenergy 7 (3), 488–496.
Nzediegwu, C., Prasher, S., Elsayed, E., Dhiman, J., Mawof, A., Patel, R., 2020. Biochar applied to soil under wastewater irrigation remained environmentally viable for the second season of potato cultivation. J. Environ. Manag. 254.
Quik, J.T.K., Velzeboer, I., Wouterse, M., Koelmans, A.A., van de Meent, D., 2014. Heteroaggregation and sedimentation rates for nanomaterials in natural waters. Water Res. 48, 269–279.
Qian, L., Zhang, W., Yan, J., Han, L., Gao, W., Liu, R., et al., 2016. Effective removal of heavy metal by biochar colloids under different pyrolysis temperatures. Bioresource Technol. 206, 217–224.
Ravi, S., Sharratt, B.S., Li, J., Olshevski, S., Meng, Z., Zhang, J., 2016. Particulate matter emissions from biochar-amended soils as a potential trade off to the negative emission potential. Sci. Rep-UK 6, 35984.
Rosa, J.M., Rosado, M., Paneque, M., Miller, A.Z., Knicker, H., 2018. Effects of aging under field conditions on biochar structure and composition: implications for biochar stability in soils. Sci. Total Environ. 613, 969–976.
Spokas, K.A., Novak, J.M., Masiello, C.A., Johnson, M.G., Colosky, E.C., Ippolito, J.A., et al., 2014. Physical disintegration of biochar: an overlooked process. Environ. Sci. Technol. Lett. 1 (8), 326–332.
Song, B., Chen, M., Zhao, L., Qiu, H., Cao, X., 2019. Physicochemical property and colloidal stability of micron- and nano-particle biochar derived from a variety of feedstock sources. Sci. Total Environ. 661, 685–695.
Shi, Y., 2011. China's resources of biomass feedstock. Eng. Sci. 2, 16–22 (in Chinese).
Tang, Z., Wu, L., Luo, Y., Peter, C., 2009. Size fractionation and characterization of nanocolloidal particles in soils. Environ. Geochem. Health. 31 (1), 1–10.
Wang, L., Yang, X., Wang, Q., Zeng, Y., Ding, L., Jiang, W., 2017. Effects of ionic strength and temperature on the aggregation and deposition of multi-walled carbon nanotubes. J. Environ. Sci. 51, 248–255.
Wang, L., Qin, L., Lv, X., Jiang, M., Zou, Y., 2018. Progress in researches on effect of iron promoting accumulation of soil organic carbon. Acta Pedol. Sinica. doi:10.11766/trxb201802260035, (in Chinese).
Wang, S., Sun, B., Li, C., Li, Z., Ma, B., 2018a. Runoff and soil erosion on slope cropland: a review. J. Resour. Ecol. 9 (5), 461–470.
Wang, X., Yang, Z., Liu, X., Lin, W., Yang, Y., Liu, Z., et al., 2016. Effects of different forms of Fe and Al oxides on soil aggregate stability in mid-subtropical mountainous area of southern China. Acta Ecol. Sin. doi:10.5846/stxb201408021542, (in Chinese).
Wang, Y., Zhang, W., Shang, J., Shen, C.Y., Joseph, S.D., 2019. Chemical aging changed aggregation kinetics and transport of biochar colloids. Environ. Sci. Technol. 53 (14), 8136–8146.
Xu, R., Duanmu, Y., Wen, L., Tang, W., Bi, S., 2001. Computer simulation of aluminum speciation in soil water equilibria with mineral phase basaluminite. Acta Sci. Circum. doi:10.13671/j.hjkxxb.2001.s1.013, (in Chinese).
Yang, W., Shang, J., Prabhakar, S., Li, B., Liu, K., Markus, F., 2019. Colloidal stability and aggregation kinetics of biochar colloids: effects of pyrolysis temperature, cation type, and humic acid concentrations. Sci. Total Environ. 658, 1306–1315.
Yi, P., Pignatello, J.J., Uchimiya, M., White, J.C., 2015. Heteroaggregation of cerium oxide nanoparticles and nanoparticles of pyrolyzed biomass. Environ. Sci. Technol. 49 (22), 13294–13303.